

Subwavelength silicon through-hole arrays as an all-dielectric broadband terahertz gradient index metamaterial

Sang-Gil Park, Kanghee Lee, Daehoon Han, Jaewook Ahn, and Ki-Hun Jeong

Citation: [Applied Physics Letters](#) **105**, 091101 (2014); doi: 10.1063/1.4894054

View online: <http://dx.doi.org/10.1063/1.4894054>

View Table of Contents: <http://scitation.aip.org/content/aip/journal/apl/105/9?ver=pdfcov>

Published by the [AIP Publishing](#)

Articles you may be interested in

[Cavity enhanced terahertz modulation](#)

Appl. Phys. Lett. **104**, 103508 (2014); 10.1063/1.4868416

[All-dielectric three-dimensional broadband Eaton lens with large refractive index range](#)

Appl. Phys. Lett. **104**, 094101 (2014); 10.1063/1.4867704

[Tuning the effective refractive index of a thin air gap region sandwiched by metallic metamaterials by lateral displacements](#)

J. Appl. Phys. **113**, 243103 (2013); 10.1063/1.4812384

[Pneumatically switchable graded index metamaterial lens](#)

Appl. Phys. Lett. **102**, 031904 (2013); 10.1063/1.4788918

[Transmission properties of terahertz pulses through an ultrathin subwavelength silicon hole array](#)

Appl. Phys. Lett. **86**, 141102 (2005); 10.1063/1.1897842

A row of tablets displaying the cover of the journal 'Computing: Science & Engineering'. The covers feature a colorful, abstract circular pattern. The text 'computing' is in a large, bold, orange font, with 'SCIENCE & ENGINEERING' in a smaller, white font below it. Below the image, the text 'AIP's JOURNAL OF COMPUTATIONAL TOOLS AND METHODS. AVAILABLE AT MOST LIBRARIES.' is displayed in a large, white, sans-serif font.

Subwavelength silicon through-hole arrays as an all-dielectric broadband terahertz gradient index metamaterial

Sang-Gil Park,^{1,2} Kanghee Lee,^{2,3} Daehoon Han,^{2,3} Jaewook Ahn,^{2,3} and Ki-Hun Jeong^{1,2,a)}

¹Department of Bio and Brain Engineering, Korea Advanced Institute of Science and Technology (KAIST), 291 Daehak-ro, Yuseong-gu, Daejeon 305-701, South Korea

²KAIST Institute for Optical Science and Technology, Korea Advanced Institute of Science and Technology (KAIST), 291 Daehak-ro, Yuseong-gu, Daejeon 305-701, South Korea

³Department of Physics, Korea Advanced Institute of Science and Technology (KAIST), 291 Daehak-ro, Yuseong-gu, Daejeon 305-701, South Korea

(Received 8 June 2014; accepted 8 July 2014; published online 2 September 2014)

Structuring at subwavelength scales brings out artificial media with anomalous optical features called metamaterials. All-dielectric metamaterials have high potential for practical applications over the whole electromagnetic spectrum owing to low loss and optical isotropy. Here, we report subwavelength silicon through-hole arrays as an all-dielectric gradient index metamaterial with broadband THz operation. The unit cell consists of a single subwavelength through-hole on highly resistive monocrystalline silicon. Depending on the fill-factor and period, the effective index was linearly modulated at 0.3–1.6 THz. The experimental results also demonstrate silicon gradient refractive index (Si-GRIN) lenses with parabolic index profiles through the spatial modification of a single unit cell along the radial direction. Si-GRIN lenses either focus 0.4–1.6 THz beam to the diffraction-limit or serve as a flat and thin solid immersion lens on the backside of THz photoconductive antenna for highly efficient pulse extraction. This all-dielectric gradient index metamaterial opens up opportunities for integrated THz GRIN optics. © 2014 AIP Publishing LLC.

[<http://dx.doi.org/10.1063/1.4894054>]

Metamaterials, i.e., artificial media structured at subwavelength scale, drive a new paradigm for photonic materials across the full range of electromagnetic spectrum. They exhibit many intriguing features such as optical magnetism, double-negative index,¹ abnormal high-index,² optical chirality,³ tunable transmission,^{4–6} and gradient-index.⁷ Moreover, they allow THz photonic devices such as beam deflectors,⁸ bandpass filters,^{9,10} phase modulators,¹¹ perfect absorbers,^{12,13} thin-film sensors,¹⁴ and gradient index lenses.¹⁵ However, conventional metamaterials still rely upon subwavelength metallic resonators and thus inherently suffer from significant conduction loss, narrow bandwidth, and strong optical anisotropy due to their geometric asymmetry. Recently, diverse alternative approaches have been demonstrated such as silk composite metamaterials¹⁶ and all-dielectric metamaterials with artificial magnetism or near-zero index.^{17–19} In particular, all-dielectric metamaterials apparently have both low absorption and optical isotropy, which facilitate the spatial index variation in transformation optics such as electromagnetic cloaking^{20,21} and an extreme-angle lens.²² Here, we report an all-dielectric gradient-index metamaterial with low absorption and broadband operation based on subwavelength silicon through-hole arrays. The effective index can be precisely controlled by the geometric parameters of subwavelength through-hole arrays, which allow the implementation of a gradient index lens with low dispersion in a broad THz frequency range.

The all-dielectric gradient-index metamaterial contains subwavelength through-hole arrays in a hexagonal lattice on

monocrystalline silicon (Fig. 1(a)). The hexagonal arrangement provides not only a high relative fraction of air for a long-range modulation of the effective index but also the mechanical stability. The unit cell of a single subwavelength through-hole can be mainly altered by the period and the fill-factor (FF), i.e., an area ratio of silicon in the unit cell (Fig. 1(b)). High-resistivity monocrystalline silicon with low absorption and low dispersion serves as a bulk medium for the index modulation. The gradient index metamaterial was numerically confirmed by observing the deflection of a beam incident on a planar metamaterial with a finite-difference time-domain (FDTD) method. The diameters of subwavelength through-hole arrays vary along x-axis with a period of 120 μm and a thickness of 100 μm in order to construct a constant spatial gradient in index. The wave becomes deflected by different phase advances propagating through the gradient index metamaterial. The electric field distributions were acquired on $y=0$ and $x=800\ \mu\text{m}$ at 1 THz and the gradient index metamaterial was indicated by white dash lines (Fig. 1(c)). The calculated results clear show uniform deflection of the wave towards x-axis and uniform electric field distribution along y-axis. No significant diffraction was observed. Moreover, the deflection angle shows a good agreement with a theoretical value of 13.6° as shown in the black dash lines of Fig. 1(c). This uniform deflection indicates that the unit cell arrays with discrete indices can serve as a well-defined effective medium.

The subwavelength silicon through-hole arrays may exhibit guided resonance modes in Bragg regime.²³ In particular, the effective index shows a normal dispersion behavior due to the lowest-order resonance. The normal dispersion region was experimentally investigated in subwavelength

^{a)}Author to whom correspondence should be addressed. Electronic mail: kjeong@kaist.ac.kr

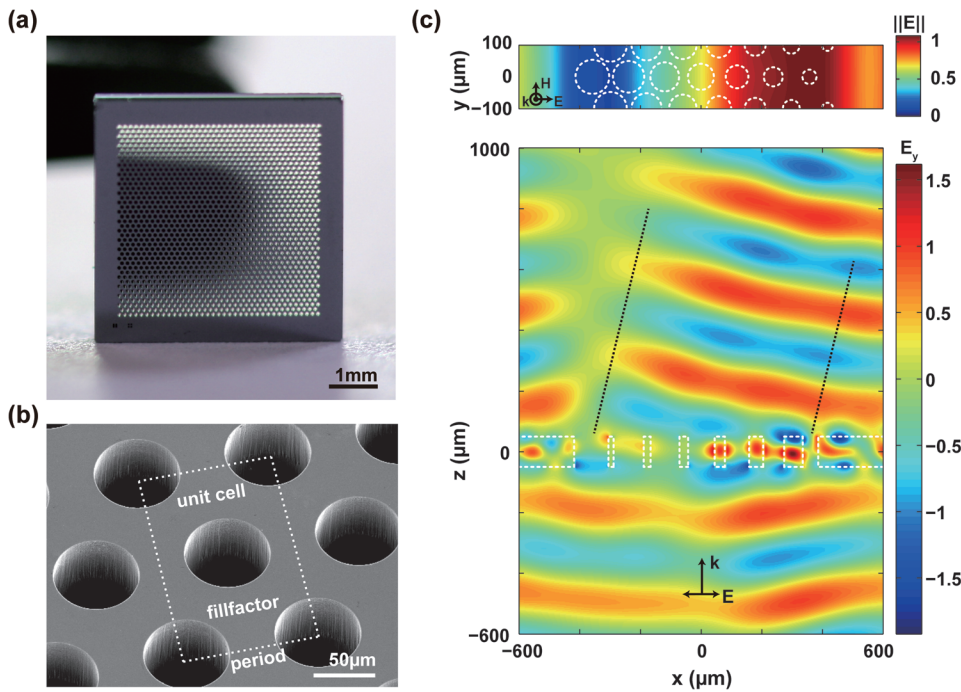


FIG. 1. Subwavelength silicon through-hole arrays as an all-dielectric broadband THz gradient index metamaterial. (a) A photographic image of a high resistivity monocrystalline silicon slab with subwavelength through-hole arrays. (b) A perspective SEM image of the unit cells in a hexagonal lattice on the silicon slab. (c) Uniform deflection of THz beam passing through subwavelength through-hole arrays with a constant spatial gradient in index. The linearly increasing effective index deflects the wave fronts without significant distortion. Subwavelength silicon through-hole arrays apparently serve as an all-dielectric THz gradient index metamaterial.

silicon through-hole arrays for a broadband THz gradient index metamaterial. In the experiment, both the effective index and the normal dispersion were precisely modulated by changing the period and the fill-factor of a unit cell. The subwavelength silicon through-hole arrays were monolithically fabricated by using photolithography and deep-reactive-ion etching (DRIE) on a 6-in. silicon wafer. (See supplementary material for further detail.²⁴) THz time-domain signals were measured by THz-time domain spectroscopy (TDS) in a dry environment. The measured effective indices were extracted from the time-domain signals at 0.3–1.6 THz by using a numerical iterative method²⁵ and then compared with the numerically calculated values by using an S-parameter retrieval method.²⁶ Both the results clearly show the effective indices increase with the fill-factor at 0.3–1.6 THz (Figs. 2(a) and 2(b)). The index modulation was also examined by the pulse delays in THz time-domain signals (Fig. S1). The effective index is linearly modulated by 0.1 RIU per 5% FF in 0.3–1.6 THz frequency range. In

particular, the normal dispersion shows ~ 0.6 RIU/THz for the period of $110 \mu\text{m}$. This normal dispersion obviously decreases as the period decreases (Fig. 2(c)); the effective index at 1.5 THz significantly decreases with the period, whereas the effective index at 0.5 THz is relatively constant. Note that the lower dispersion with the smaller period results from the blue shift of the lowest guided resonance. The small period is apparently crucial for low-dispersive THz materials. However, the minimum period is still limited by the slab thickness due to the maximum aspect ratio of a silicon DRIE process, normally $\sim 20:1$. As a result, the change in fill-factor with the minimum allowable period realizes the index modulation with low dispersion for practical applications.

The subwavelength silicon through-hole arrays with low dispersion were further utilized for a silicon gradient refractive index (Si-GRIN) lens with broadband THz operation. The unit cells under a constant period of $120 \mu\text{m}$ clearly show a constant rate of index-change at broadband THz frequencies as the fill-factor increases (Fig. 3(a)). In GRIN

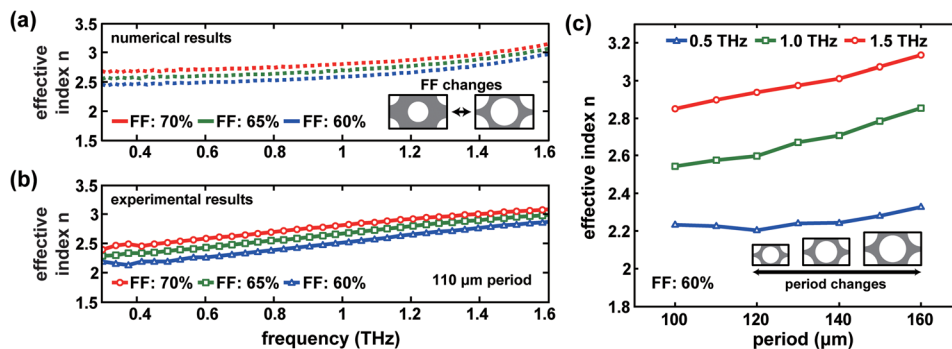


FIG. 2. Modulation of effective index and dispersion depending on the geometric parameters. Calculated (a) and measured (b) effective refractive indices of the subwavelength through-hole arrays with different fill-factors and a constant period of $110 \mu\text{m}$. The effective index linearly increases by 0.1 RIU per 5% FF in 0.3–1.6 THz broadband frequencies with small normal dispersion of ~ 0.6 RIU/THz. (c) The measured indices of the subwavelength silicon through-hole arrays with the different periods and a constant 60% FF. The normal dispersion moderately decreases with the period due to the blue shift of the guided resonance.

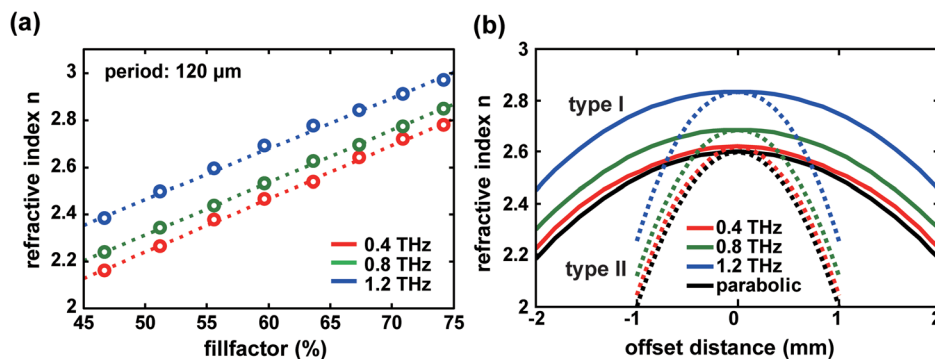


FIG. 3. Parabolic index profiles of Si-GRIN lens. (a) Refractive index of the subwavelength silicon through-hole arrays at different frequencies depending on the fill-factor with a constant $120 \mu\text{m}$ period. As a prerequisite for broadband gradient optics, the refractive index constantly increases with the fill-factor over 0.4–1.2 THz range. (b) Parabolic spatial gradients in effective index for Si-GRIN lenses along the radial direction. Two types of Si-GRIN lenses were designed for a beam focusing lens in free-space (type I, solid line) and a solid immersion lens on photoconductive antenna (type II, dash line), respectively. The parabolic index profiles along the offset distance (a distance from the center) are completely preserved at broadband frequencies.

optics, the lens power is determined by the spatial gradient in effective index. The constant index variation, i.e., parallel slopes shown in Fig. 3(a), at broadband THz frequencies thus allow the broadband operation of Si-GRIN lens and thereafter the effective indices of individual unit cells were spatially modified in order to obtain a parabolic profile along the radial direction. Two different types of Si-GRIN lens were designed for a positive lens in free-space (type I, $D = 4 \text{ mm}$, $F/2$, solid line in Fig. 3(b)) and a solid immersion lens (type II, $D = 2 \text{ mm}$, $F/0.7$, dash line in Fig. 3(b)). The index profiles of both Si-GRIN lenses clearly show parabolic parallels in effective index along the radial direction for the broadband operation at THz frequencies (Fig. 3(b)).

Both Si-GRIN lenses were also fabricated by using the same procedure for the subwavelength silicon through-hole arrays (Fig. 4(a)). THz beam focusing through the Si-GRIN lens (type I) was measured by scanning a probe beam on THz-TDS with a spatial resolution of $\sim 40 \mu\text{m}$ and a maximum scan range of $\pm 5.7 \text{ mm}$ within 5% error. (See

supplementary material for further detail.²⁴) This direct measurement allows the clear observation of a focused beam profile by reducing the alignment errors from other THz optical elements such as parabolic mirrors (Fig. 4(b)). THz beam focusing through the Si-GRIN lens increases the maximum spectral intensity of 2D THz intensity map. The maximum enhancement is 8.3-folds at 0.68 THz, whereas the Fresnel reflection loss of $\sim 36\%$ exists at both air-silicon interfaces of the Si-GRIN lens. Note that the Fresnel reflection loss of Si-GRIN lens becomes substantially low compared to 51% loss in bare silicon ($n_{\text{Si}} = 3.4$) due to a low index nature of subwavelength silicon through-hole arrays ($n_{\text{center}} = 2.6\text{--}2.8$). The intensity distribution of focused THz beam on a focal image plane was then reconstructed by mapping the measured THz electric fields at different positions. (Fig. 4(c), inset). The beam intensity map shows the Gaussian beam profile without substantial distortion, which clearly demonstrates the subwavelength silicon through-hole arrays serve as a homogeneous medium during beam

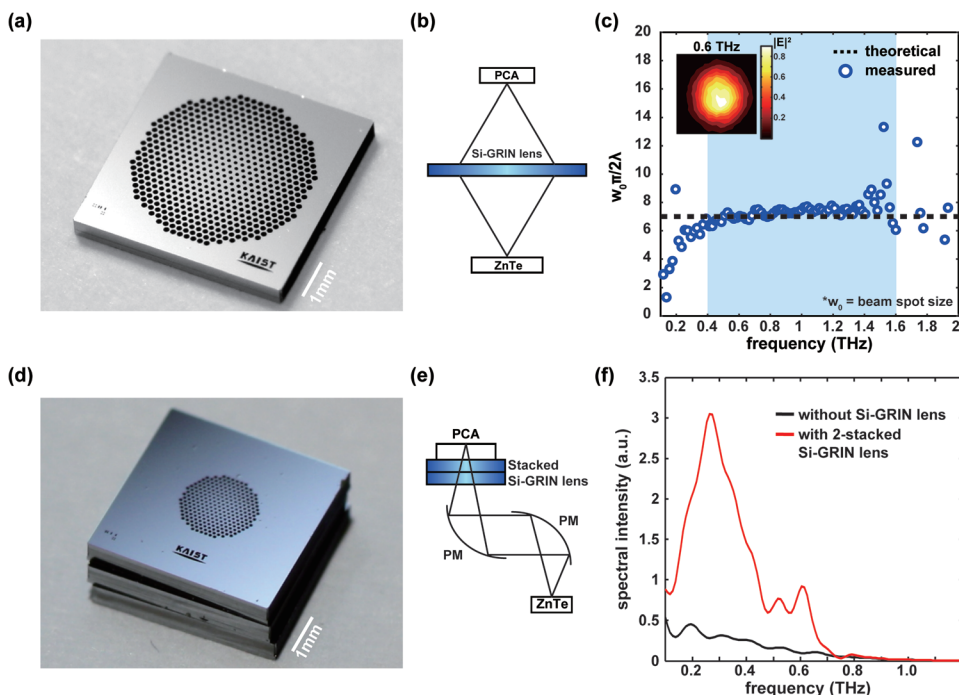


FIG. 4. Silicon gradient-index lenses for THz beam focusing and THz pulse extraction. (a) A photographic image of the Si-GRIN lens (type I, lens diameter: 4 mm , $F/2$) with a spatial gradient in index along the radial direction by changing the fill-factor of the unit cell. (b) The schematic diagram of THz TDS based measurement set-up for THz beam focusing. (c) Diffraction-limited beam focusing. The focused spot sizes w_0 , normalized to the wavelength λ , correspond to the diffraction limits at 0.4–1.6 THz frequencies. The inset demonstrates the measured Gaussian beam profile at the focal spot of 0.6 THz. (d) A photographic image of the solid immersion stacked Si-GRIN lenses (type II, lens diameter: 4 mm , $F/0.7$). (e) The schematic diagram of THz TDS based measurement set-up for THz pulse extraction. (f) Comparison between THz pulse intensities emitted from a PCA with and without the stacked Si-GRIN lenses.

focusing. The THz beam focused by the Si-GRIN lens is diffraction-limited at 0.4–1.6 THz, which indicates the focal length of Si-GRIN lens has a good agreement with the designed value, i.e., $F/2$. The operating bandwidth of 1.2 THz remarkably surpasses that of metallic metamaterials.

The planar configuration of Si-GRIN lens facilitates the vertical integration between the lenses and other THz optics. The stacked Si-GRIN lenses (type II) can be further utilized as a solid immersion lens (SIL) on the backside of THz photoconductive antenna (PCA) for highly efficient THz pulse extraction (Fig. 4(d)). In conventional THz emitter, the only 5% of THz radiation is extracted due to total internal reflection inside a high index PCA substrate and therefore a thick and bulky silicon dome lens is necessary for highly efficient extraction of THz radiation. THz pulse extraction through SIL of two stacked Si-GRIN lenses was measured by using conventional THz-TDS (Fig. 4(e)). THz pulses emitted from the THz PCA were collected and focused on ZnTe crystal by parabolic mirrors. The measured results demonstrate the stacked Si-GRIN lenses serve as a SIL for highly efficient THz pulse extraction on the backside of PCA (Fig. 4(f)). The spectral intensity is substantially enhanced by 10.3 times at 0.26 THz in maximum and the average enhancement is 4.2 times from 0.1 to 1 THz.

This Si-GRIN lens has high performance and cost-effectiveness, compared to the conventional THz lens. First, Si-GRIN lens provides sufficiently low dispersion that enables the direct time-domain measurement of a focused THz beam due to the small increase in pulse-width (Fig. S4). The group dispersion can be further reduced by decreasing the thickness or the period of Si-GRIN lens. Next, the lens power of $F/0.7\text{--}2$ is highly comparable to those from conventional parabolic mirrors, i.e., typically $F/2\text{--}3$. The focused beam is also highly confined within a diffraction limit through Si-GRIN lens with other measurement (Fig. S5). Finally, Si-GRIN lens is highly cost-effective due to the monolithic fabrication with high yield unlike conventional THz optics such as parabolic mirrors or silicon dome lenses.

To be concluded, this work has demonstrated the subwavelength silicon through-hole arrays as a broadband THz gradient index metamaterial. This THz material affords the linear index modulation of low absorptive silicon by changing a fill-factor of a unit cell under a constant period. In particular, this gradient index metamaterial has low dispersion at broadband THz frequencies, which can open up opportunities for developing diverse gradient-index (GRIN) optics

including beam focusing or solid immersion lens at broadband THz frequencies.

Thanks to Professor B. Min for valuable discussion. This work was supported by the Ministry of Science, ICT & Future Planning grant funded by Korea government (2013035236, 2013050154, and 2012M3A6A6054199).

- ¹O. Paul, C. Imhof, B. Reinhard, R. Zengerle, and R. Beigang, *Opt. Express* **16**(9), 6736 (2008).
- ²M. Choi, S. H. Lee, Y. Kim, S. B. Kang, J. Shin, M. H. Kwak, K. Y. Kang, Y. H. Lee, N. Park, and B. Min, *Nature* **470**(7334), 369 (2011).
- ³S. Zhang, Y. S. Park, J. S. Li, X. C. Lu, W. L. Zhang, and X. Zhang, *Phys. Rev. Lett.* **102**(2), 023901 (2009).
- ⁴L. Ju, B. S. Geng, J. Horng, C. Girit, M. Martin, Z. Hao, H. A. Bechtel, X. G. Liang, A. Zettl, Y. R. Shen, and F. Wang, *Nat. Nanotechnol.* **6**(10), 630 (2011).
- ⁵H. T. Chen, J. F. O'Hara, A. K. Azad, A. J. Taylor, R. D. Averitt, D. B. Shrekenhamer, and W. J. Padilla, *Nat. Photonics* **2**(5), 295 (2008).
- ⁶H. T. Chen, W. J. Padilla, J. M. O. Zide, A. C. Gossard, A. J. Taylor, and R. D. Averitt, *Nature* **444**(7119), 597 (2006).
- ⁷D. R. Smith, J. J. Mock, A. F. Starr, and D. Schurig, *Phys. Rev. E* **71**(3), 036609 (2005).
- ⁸X. Q. Zhang, Z. Tian, W. S. Yue, J. Q. Gu, S. Zhang, J. G. Han, and W. L. Zhang, *Adv. Mater.* **25**(33), 4567 (2013).
- ⁹O. Paul, R. Beigang, and M. Rahm, *Opt. Express* **17**(21), 18590 (2009).
- ¹⁰N. R. Han, Z. C. Chen, C. S. Lim, B. Ng, and M. H. Hong, *Opt. Express* **19**(8), 6990 (2011).
- ¹¹H. T. Chen, W. J. Padilla, M. J. Cich, A. K. Azad, R. D. Averitt, and A. J. Taylor, *Nat. Photonics* **3**(3), 148 (2009).
- ¹²C. M. Watts, X. L. Liu, and W. J. Padilla, *Adv. Mater.* **24**(23), Op98 (2012).
- ¹³H. Tao, N. I. Landy, C. M. Bingham, X. Zhang, R. D. Averitt, and W. J. Padilla, *Opt. Express* **16**(10), 7181 (2008).
- ¹⁴J. F. O'hara, R. Singh, I. Brener, E. Smirnova, J. G. Han, A. J. Taylor, and W. L. Zhang, *Opt. Express* **16**(3), 1786 (2008).
- ¹⁵J. Neu, B. Krolla, O. Paul, B. Reinhard, R. Beigang, and M. Rahm, *Opt. Express* **18**(26), 27748 (2010).
- ¹⁶H. Tao, J. J. Amsden, A. C. Strikwerda, K. Fan, D. L. Kaplan, X. Zhang, R. D. Averitt, and F. G. Omenetto, *Adv. Mater.* **22**(32), 3527 (2010).
- ¹⁷P. Moitra, Y. M. Yang, Z. Anderson, I. I. Kravchenko, D. P. Briggs, and J. Valentine, *Nat. Photonics* **7**(10), 791 (2013).
- ¹⁸J. C. Ginn, I. Brener, D. W. Peters, J. R. Wendt, J. O. Stevens, P. F. Hines, L. I. Basilio, L. K. Warne, J. F. Ihlefeld, P. G. Clem, and M. B. Sinclair, *Phys. Rev. Lett.* **108**(9), 097402 (2012).
- ¹⁹Q. Zhao, J. Zhou, F. L. Zhang, and D. Lippens, *Mater. Today* **12**(12), 60 (2009).
- ²⁰D. Schurig, J. J. Mock, B. J. Justice, S. A. Cummer, J. B. Pendry, A. F. Starr, and D. R. Smith, *Science* **314**(5801), 977 (2006).
- ²¹R. Liu, C. Ji, J. J. Mock, J. Y. Chin, T. J. Cui, and D. R. Smith, *Science* **323**(5912), 366 (2009).
- ²²N. Kundtz and D. R. Smith, *Nat. Mater.* **9**(2), 129 (2010).
- ²³S. H. Fan and J. D. Joannopoulos, *Phys. Rev. B* **65**(23), 235112 (2002).
- ²⁴See supplementary material at <http://dx.doi.org/10.1063/1.4894054> for the details of fabrication and measurement.
- ²⁵L. Duvillelet, F. Garet, and J. L. Coutaz, *IEEE J. Sel. Top. Quantum* **2**(3), 739 (1996).
- ²⁶D. R. Smith, D. C. Vier, T. Koschny, and C. M. Soukoulis, *Phys. Rev. E* **71**(3), 036617 (2005).